PHYSICAL REVIEW C VOLUME 25, NUMBER 2 FEBRUARY 1982

Energy dependence of fusion cross section for $^{28}Si + ^{12}C$ by evaporation residue measurements

K. T. Lesko, D.-K. Lock, A. Lazzarini, R. Vandenbosch, V. Metag,* and H. Doubre†
Nuclear Physics Laboratory, University of Washington, Seattle, Washington 98195
(Received 25 September 1981)

The excitation function for production of evaporation residues from the fusion of $^{28}Si + ^{12}C$ has been studied in two experiments. In the first experiment the γ-ray yields of transitions populating final state evaporation residues were measured, thereby allowing a detailed study of the bombarding energy dependence of the production of specific isotopes. More accurate absolute cross sections for evaporation residue production were measured at several energies with a gas proportional ΔE solid state E telescope. In this manner absolute cross sections were determined against which the γ-ray data could be normalized. The fusion cross section is found to vary smoothly with bombarding energy. Further, absolute cross sections agree well with model predictions currently in vogue.

[NUCLEAR REACTIONS Fusion, measured $\sigma_{fusion}(E)$; $^{12}C + ^{28}Si$, $18.4 \leq E_{c.m.} \leq 35$ MeV. Compared with entrance channel and level density limitation models.]

I. INTRODUCTION

Earlier reports of pronounced structure in the energy dependence of elastic and inelastic scattering at backward angles in the $^{12}C + ^{28}Si$ system have been interpreted by various authors[1,2] as evidence for the presence of resonances in the heavy ion system. More recently there have been published data that indicate a resonance interpretation is not supported by the energy dependence of the elastic scattering[3] at $\theta_{c.m.} = 90°$ and also by the total integrated yield of the 2^+ state in ^{28}Si at 1.78 MeV.[4] The integrated back-angle yield of C and O products, however, has been recently reported to exhibit structure over the center of mass (c.m.) energy range between 30 and 40 MeV.[5] We report here on measurements, made simultaneouly with those of Ref. 4, of the energy dependence of the fusion cross section as inferred by the detection of final state evaportation residues (ER). Because of unitarity considerations one expects that any real resonant structure observable in massive exit channels such as elastic and inelastic scattering and transfer channels[6] should also reflect itself in the energy dependence of fusion. This has been shown[7,8] to be the case with lighter systems involving ^{12}C and ^{16}O.

II. EXPERIMENTAL METHOD

A. γ-ray experiment

The details of the γ-ray measurement have been presented elsewhere.[4] Briefly, two Ge(Li) detectors were positioned at 90° and 144° relative to the ^{12}C beam. The target consisted of 100 $\mu g/cm^2$ ^{28}Si on a thick tantalum backing. The target and scattering chamber were electrically isolated from the system and served as a Faraday cup for the beam integration. In addition, the backing served as a check in cross section normalization by the observation of Coulomb excitation of the tantalum.

A typical Ge(Li) γ-ray spectrum is presented in Fig. 1. The lines which are labeled correspond to known transitions in evaporation residues produced in the fusion reaction. The bulk of the ER yield is accounted for by the 11 transitions presented in Table I. Our reported fusion excitation function was obtained by summing the listed transitions.

B. Particle measurement

The telescope measurements were made with a gas proportional position sensitive ΔE solid state E telescope. A 90—10% argon-methane mixture

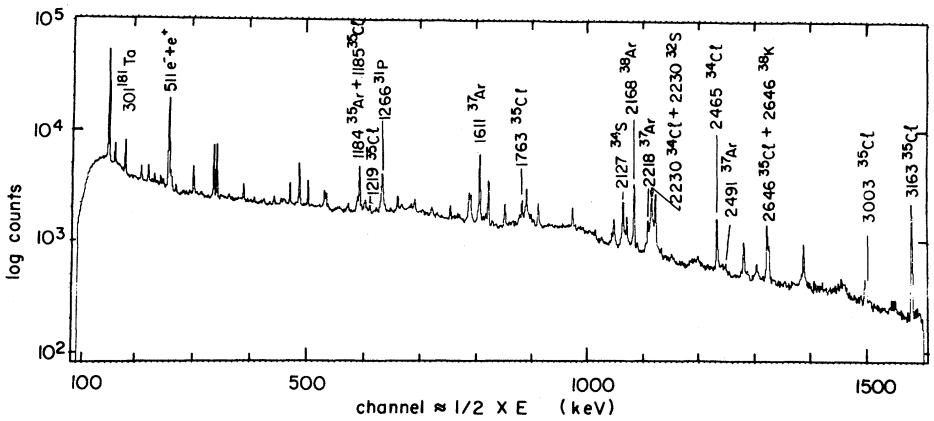

FIG. 1. Gamma-ray spectrum obtained at $E_L(^{12}C)=48.5$ MeV. Identifications of the prominent transitions are shown.

was used at a pressure of ≈ 30 Torr for the ΔE element. The details of the counter have been presented in the literature.[9] Position sensitivity was obtained by measuring the time difference between the energy signal in the solid state detector and the signal on the proportional wire. The difference in arrival times reflects the electron drift velocity in the gas ΔE element of the telescope. A mask with four slits, each of which subtended $\Delta\theta \approx 0.32°$, $\Delta\phi \approx 1.0°$, was placed in front of the counter. The slits themselves were separated by 0.85°. In this configuration four different angles could be monitored simultaneously.

Twenty two-point angular distributions were taken of the fusion ER from $\theta_{lab}=2.5°-18.0°$. The energy steps taken in this measurement were not as fine as those for the γ-ray measurements. They were chosen by considering the presence of the energy-dependent structure reported in the elastic and inelastic scattering measurements.[1-3]

To improve the performance of the telescope and also to reduce the angular range over which fusion ER were produced, the reaction was kinematically inverted. A 50 μg/cm^2 isotopic ^{12}C target was bombarded with a ^{28}Si beam from the University of Washington tandem Van de Graaff. Figure 2 presents a typical ΔE-E contour plot obtained in these measurements. The charge resolution was rather poor; however, for the purposes of our interests, it was sufficient to resolve the fusion ER group from beamlike particles. In Fig. 2 are shown lines indicating the expected location of various elemental lines; the lines are taken from known dE/dx relationships among the elements in this mass region.[10] We estimate our resolution to be $\Delta Z \approx 1.5$ as determined by taking selected E cuts of the ΔE spectrum. Excluding all $Z \leq 14$ from the integration of the fusion cross section is not expected to affect the magnitude of the measured cross section appreciably ($\leq 5\%$); this is borne out in simple cascade calculations we performed at the highest beam energy studied here, where production of fusion ER with $Z \leq 14$ is expected to be most important.

TABLE I. Strong γ-ray transitions observed in the $^{12}C + ^{28}Si$ reaction.

Nucleus	Transition ($J_i^\pi \rightarrow J_f^\pi$)	E_γ (keV)
^{34}Cl	$(4^+ \rightarrow 3^+)$	2230
^{34}Cl	$(2^+ \rightarrow 3^+)$	2465
^{35}Cl	$(\frac{5}{2}^+ \rightarrow \frac{3}{2}^+)$	1763
^{35}Cl	$(\frac{7}{2}^+ \rightarrow \frac{3}{2}^+)$	2646
^{35}Cl	$(\frac{7}{2}^+ \rightarrow \frac{3}{2}^+)$	3163
^{38}Ar	$(2^+ \rightarrow 0^+)$	2168
^{34}S	$(2^+ \rightarrow 0^+)$	2127
^{31}P	$(\frac{3}{2}^+ \rightarrow \frac{1}{2}^+)$	1266
^{35}Ar	$(\frac{1}{2}^+ \rightarrow \frac{3}{2}^+)$	1184
^{37}Ar	$(\frac{7}{2}^- \rightarrow \frac{3}{2}^+)$	1611
^{37}Ar	$(\frac{7}{2}^+ \rightarrow \frac{3}{2}^+)$	2217

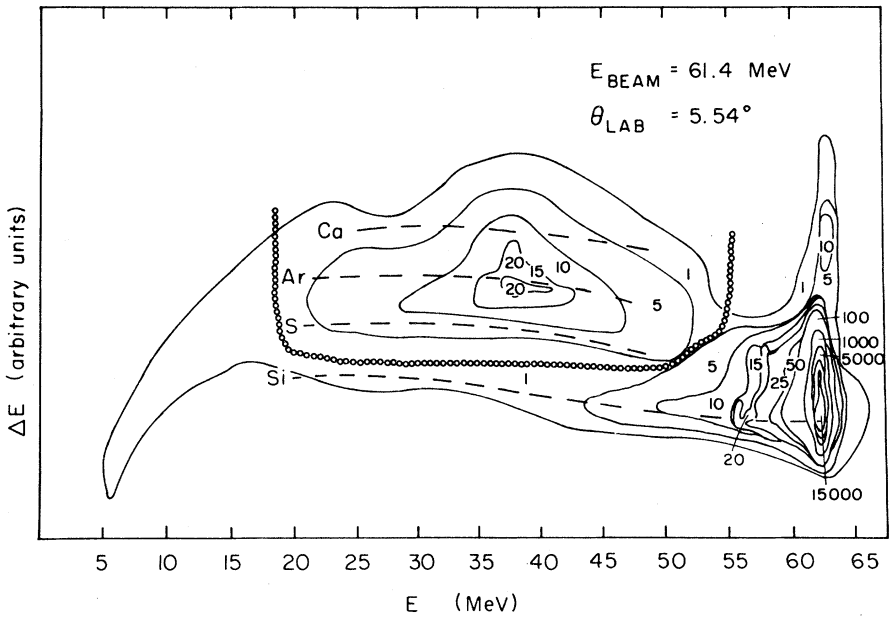

FIG. 2. Contour map of counts in the ΔE-E plane at $E_L(^{28}\text{Si})=61.4$ MeV with dashed curves to indicate expected residue yields.

III. ANALYSIS AND RESULTS

A. γ-ray measurements

The fusion-evaporation excitation function was determined by integrating the yield of the mutually exclusive γ transitions listed in Table I. The transitions indicated are expected to faithfully represent the production yield of the nuclides with the exception of the direct production of these nuclei in their ground state. These nuclides represent the bulk of the fusion-evaporation cross section, although some ER were impossible to extract because their yield reflects processes other than fusion evaporation (^{28}Si) or because the appropriate transition could not be resolved from other transitions (^{32}S).

Absolute cross sections were determined from the integrated beam current and target thickness and are believed to be good to 20%. For later analysis, however, the γ-ray data were normalized to the evaporation residue measurements. Some transitions, such as the ^{34}Cl lines, were difficult to extract because of interfering background lines. Relative cross sections in the excitation function have a precision of 3—5 % arising from counting statistics.

Figure 3 presents the energy dependence of the most copious residues labeled by their decay channel from the ^{40}Ca compound nucleus. Total cross sections were obtained from measured differential cross sections. The angular distribution of γ rays were assumed to be of the form

$$d\sigma/d\Omega = a + b\cos^2\theta \ . \tag{1}$$

The coefficients a and b are energy dependent; it

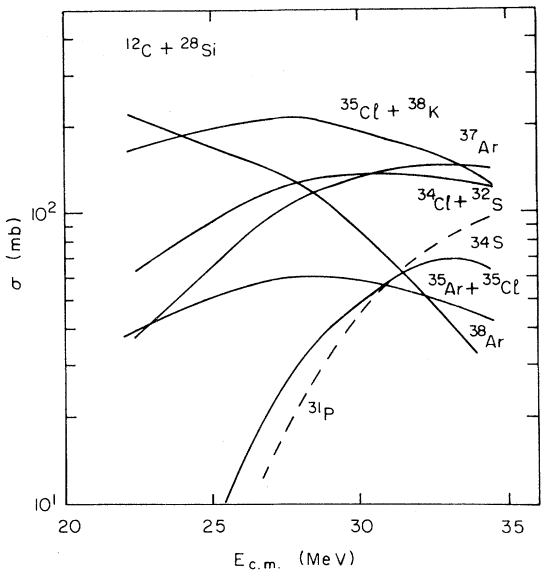

FIG. 3. Excitation functions for individual products as determined by γ-ray yields.

was assumed, however, that their ratio $\rho \equiv b/a$ was energy independent. In this manner the differential cross section at $\theta = 90°$ serves to determine the total cross section

$$\sigma(E) = \int d\sigma/d\Omega(E) d\Omega$$
$$= 4\pi (d\sigma/d\Omega)_{90°}(1+\rho/3) . \quad (2)$$

The anistropy correction, $\rho/3$ was 10%.

Figure 4 shows the measured elemental distribution of evaporation residues and compares it with evaporation model[11–14] predictions for the system at two c.m. energies. We see the agreement is good with the exception of the αn and pn channels. We shall come back to this point later. The determination of absolute cross sections for ER production from γ-ray measurements suffers from several problems. First, the production of ER in their ground states by direct particle decay is not observable. Second, the nuclides observed here are the strongest channels for $^{12}C + {}^{28}Si$, but they do not represent all final state products. These two shortcomings conspire to produce an energy dependent deficit in our measured fusion excitation function; the effect is expected to be smooth, so that our search for energy dependent intermediate structure is not compromised. We have used the evaporation model predictions to correct for this effect in our later comparisons with the particle data.

We have also looked for transitions which might originate from symmetric fission products of the compound system. Weak lines consistent with transitions in $^{20}Ne(2^+ \rightarrow 0^+)$ and $^{19}Ne(\frac{3}{2}^+ \rightarrow \frac{5}{2}^+)$ have upper limits of 15 and 7 mb, respectively. The apparent yields of both products are essentially constant with bombarding energy and are more likely to originate from oxygen impurity in the target than from fission.

B. Particle ER measurements

The angular distributions of the ER were numerically integrated to produce fusion cross sections. Typical differential cross sections are presented in Fig. 5. There is pronounced structure in the angular distributions which is particularly obvious at higher bombarding energies. This arises from the dominance of different decay modes at different angles; ER associated with α emission are peaked farther out in angle than ER products arising from single nucleon decay. Experimentally it was not possible to extend the angular distributions to an-

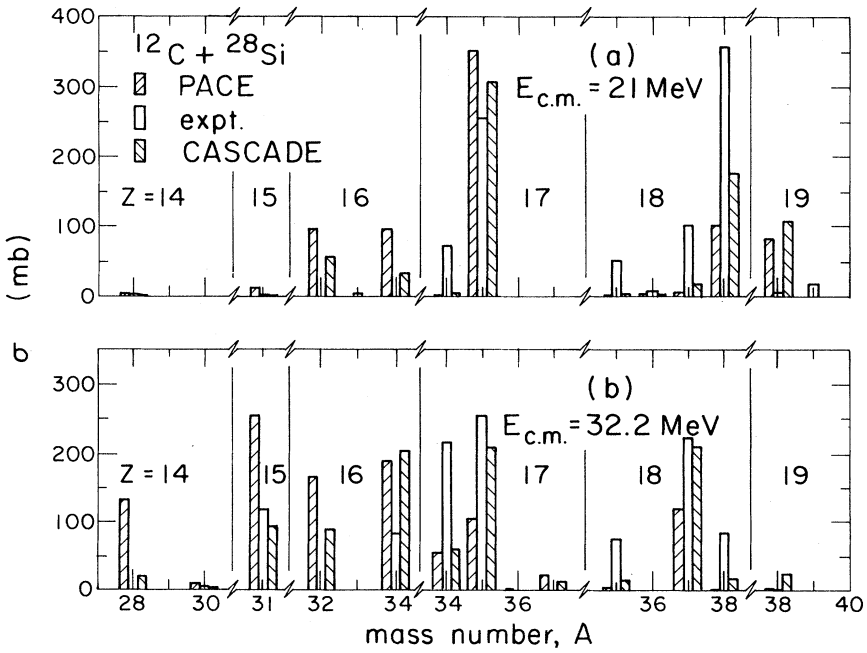

FIG. 4. Comparison of experimental nuclidic yields from γ-ray measurements with results from the statistical model codes PACE (Refs. 11 and 12) and CASCADE (Ref. 14) model yields (cross-hatched histograms) at two bombarding energies.

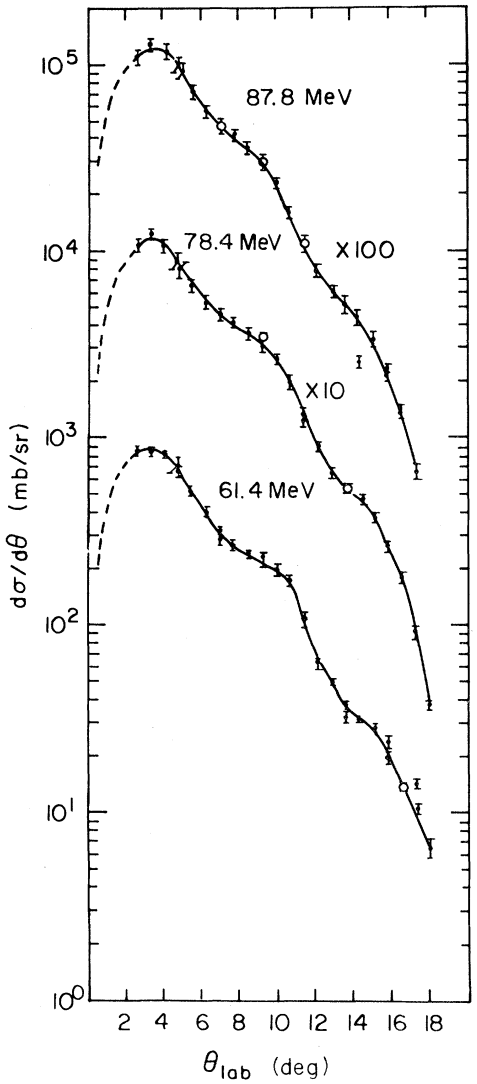

FIG. 5. Evaporation residue angular distributions at three bombarding energies. The dashed curves, used to extrapolate to zero degrees, are based on the evaporation model calculations normalized to the experimental data in the $\theta=2.5°$ to 5° to angular range. The full curves are drawn only to guide the eye.

gles smaller than $\theta_{lab}=2°$ because of geometrical limitations. The dashed lines extending to 0° in Fig. 5 are theoretical calculations for the angular distribution from the program PACE.[12] We have used this falloff to determine our total integrated yields. We estimate the uncertainties associated with this extrapolation to be small ($\approx <5\%$ of total integrated yield). This was estimated by observing the variation in cross section under different assumptions for the small angle behavior of the differential cross sections.

Absolute cross sections were obtained from elastic scattering measurements at forward angles. For all energies considered here, the elastic cross sections at angles smaller than 7° (lab) are, to a high degree of accuracy, purely Rutherford. Hence, a comparison of the ER yield to the elastic yield allows for an accurate calibration of our data. The measurements were made with frequent repeat points to allow us to normalize the data at larger angles where the elastic scattering drops well below Rutherford. The cross sections obtained are given in Table II. We present in Fig. 6 the fusion-evaporation residue excitation function. Included in the figure are the more numerous γ-ray points which have been corrected to take missed decays into account. The γ-ray data were $\approx 10\%$ lower in absolute cross section than the particle data. Since the uncertainty in the particle data is expected to be less, the γ-ray measurements have been normalized to the particle data. We note that the energy dependence of the two separate measurements corroborate each other, with the exception of the one point at $E_{c.m.}=26.8$ MeV.

As mentioned previously we have performed evaporation calculations and compared resulting individual product yields with our experimental observations. We have used three evaporation codes, PACE,[11,12] LILITA,[13] and CASCADE.[14] We find that the first two codes have a consistent tendency to overestimate the yields of channels involving α emission, e.g., ^{31}P and ^{34}S, as compared to channels involving single nucleon emission, e.g., ^{37}Ar and ^{38}Ar. The results of a calculation with PACE using its standard parameter set (Gilbert and Cameron[15] level density parameters; yrast line from a spherical liquid drop moment of inertia) have been compared with the experiment in Fig. 4. We note here that the ER particle detection measurements corroborate the discrepancies observed in the comparisons with the γ-ray data. The angular distribution of the ER contains structure arising from the difference in recoil momenta imparted to the ER by nucleon and α emission. The shoulder extending out to about 10° is due to residues which include alpha emission in their decays. The evaporation calculations with PACE predict a much larger shoulder than observed, which can be traced to the overprediction of alpha emission channels. We have made a number of attempts to improve the PACE fits by changing various parameters, such as the alpha optical potential and the moment of inertia. We also tried replacing the Gilbert and Cameron[15] level density parameters with those of Dilg

TABLE II. Evaporation residue cross sections.

$E_{c.m.}$ (MeV)	σ (mb)
18.4	559± 9
21.2	801±12
22.6	734±10
23.1	718±14
23.5	744±15
24.4	748±13
25.2	833±17
26.8	769±19
28.2	962±30

et al.[16] None of these changes gave very large improvements to the fit.

The CASCADE code gave a significantly better fit to the nuclidic yields, particularly at the higher bombarding energies. The yields calculated with this code are shown in Fig. 4. A fairly reasonable overall agreement with experiment is obtained, with occasional discrepancies approaching a factor of 2. We have not attempted to tailor the level density or optical model parameters of this code to obtain a better fit.

IV. DISCUSSION AND MODEL COMPARISONS

A. Comparison with other results

Our absolute fusion cross sections are nearly twice as large as those reported by Jordan *et al.*[7] at the lowest energy. The discrepancy between the two studies decreases with increasing bombarding energy until at the highest energy our results are nearly the same as those of the other work. We do not understand the difference, but note that our results follow more closely the qualitative behavior of the $^{12}C + {}^{29}Si$ and $^{12}C + {}^{30}Si$ systems also reported by Jordan *et al.*[17] Our results are in better qualitative agreement with standard model predictions for the energy dependence of the fusion cross section, as will be discussed below. They are also in good agreement with those of Hugi *et al.*[18]

Several studies of the back-angle elastic and inelastic scattering have revealed "resonant" structure with a periodicity of several MeV and a peak to valley ratio of $2-5$.[1-3] The arrows near the bottom of Fig. 6 indicate the positions of the peaks of the most prominent structure. The fusion excitation function does not show any structure obviously correlated with these features. The $^{24}Mg(^{16}O,^{12}C)^{28}Si$(g.s.) reaction excitation function also shows structure at energies corresponding to 30.4 and 33.6 MeV in the $^{12}C + {}^{28}Si$ channel.[19] The fact that this structure persists at the same bombarding energy for inelastic excitations[20] indicates that these structures are not due to resonances in the $^{12}C + {}^{28}Si$ exit channel.

B. Model comparisons

In Fig. 7 we plot our evaporation residue particle detection results and representative normalized γ-yield results as a function of $1/E_{c.m.}$. Also shown are the predictions of several models. The

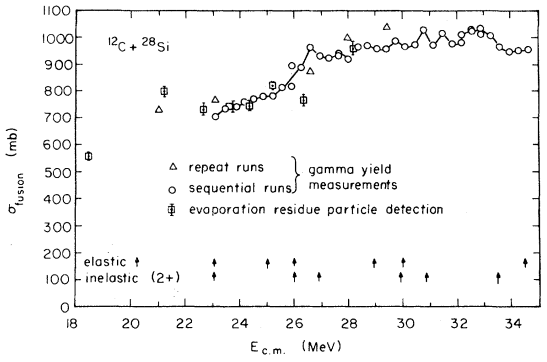

FIG. 6. Fusion cross section excitation function. The γ-yield results have been corrected for missed products and normalized to the evaporation residue particle measurements. The arrows at the bottom indicate extrema observed in the back-angle elastic and inelastic scattering excitation functions (Refs. 1 and 2). The full line through the gamma yield measurements is to guide the eye.

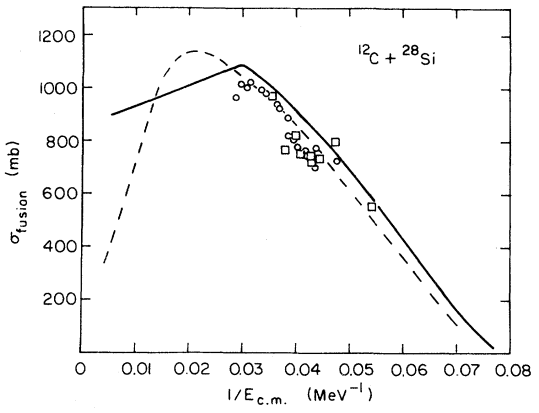

FIG. 7. Evaporation residue (squares) and representative gamma yield (circles) fusion cross sections plotted as a function of $1/E_{c.m.}$. The dashed curve is from a dynamical trajectory model calculation and the full curve is from the Bass model.

full curve is the prediction of the Bass model.[21,22] This model assumes that the tangential friction is sufficiently strong so that the sticking limit for transfer of orbital angular momentum into intrinsic rotation is reached for any impact parameters for which $r = r_{crit}$ is reached. If the total potential, including the centrifugal potential for the reduced orbital angular momentum is attractive at r_{crit}, fusion is assumed to occur. The dashed curve is the result of a classical dynamical model for fusion.[23,24] In this model the classical dynamical equations of motion are solved using both conservative and dissipative forces. The conservation forces are derived from the proximity potential[25] and the dissipative forces from proximity friction.[26] If the particle trajectory leads to trapping in a potential pocket fusion is assumed to occur. The details of the calculation are as described previously.[24] We have used half-central density radii C of 2.26 and 3.06 for ^{12}C and ^{28}Si, respectively, as deduced from electron scattering results,[27] and a diffuseness b of 1 fm. The results are shown by the full curve in Fig. 7. The results are quite similar to those for the Bass model, reflecting the fact that the proximity friction is sufficiently strong so as to usually lead to trapping if a potential pocket exits. We have also performed trajectory calculations for an improved model where a neck degree of freedom is included.[28,29] The results obtained are virtually indistinguishable from the results obtained in the results obtained in the "frozen spheres" approximation with the standard proximity potential. Our results do not extend to sufficiently high energies to show clear indication of a drop in fusion cross sections. The peak cross section of 1025 mb is somewhat lower than the values exhibited by other *sd* shell target nuclei, for which peak cross sections of almost 1200 mb are typically observed.[30,17]

There has been considerable interest lately as to whether fusion cross sections for light nuclei are limited by entrance channel or by compound nuclear limitations.[31–36] There is some evidence that for lighter systems compound nuclear level densities may play a limiting role.[33–36] To examine this question we have extracted critical angular momenta from our fusion cross sections and plotted them as a function of excitation energy in Fig. 8. Tabor *et al.*[37] have reported fusion cross section for the $^{16}O + ^{24}Mg$ system which leads to the same compound nucleus ^{40}Ca as does $^{12}C + ^{28}Si$. The critical angular momenta from their results are also shown in Fig. 8. The results from the two

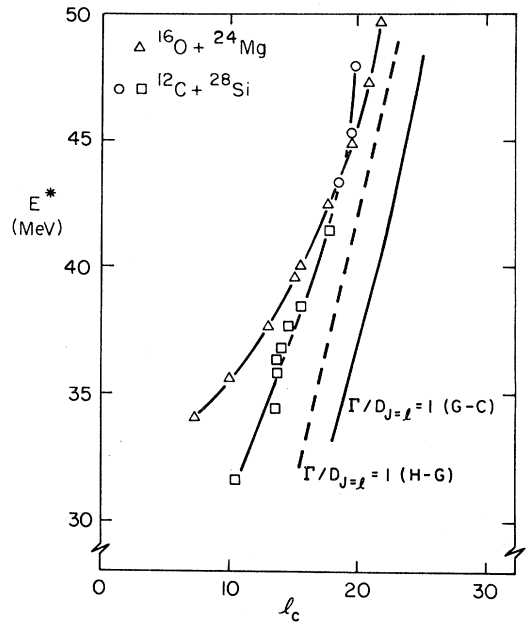

FIG. 8. Critical angular momenta for fusion as a function of compound nuclear excitation energy. The $^{16}O + ^{24}Mg$ data is from Ref. 37. The thin lines are to guide the eye. The error bar on the highest energy point for $^{12}C + ^{28}Si$ include estimated uncertainty in the normalization and correction for missed yields. The heavy full curve is calculated from the criterion that the spacing between levels of a given J be equal to the level width assuming Gilbert-Cameron level densities. The dashed curve is based on the same criterion assuming level densities obtained by the Hillman-Grover combinatorial method.

systems are quite different at low energies reflecting barrier and Q-value differences. At high energies they become quite similar with a hint that the l_c values for the two systems might cross at an excitation energy of 45 MeV. The results do not extend to high enough energy and are not sufficiently different at the highest energy to enable a conclusive statement to be made as to whether they are significantly different at the highest energy. It is interesting to note that the entrance channel model based on trajectory calculations[24] employing proximity forces predicts a crossing of the l_c values for the two systems, although this occurs at a somewhat higher excitation energy ($\sim$60 MeV) than the maximum energy reached in our experiment. If compound nuclear properties were determining the cross sections at the higher energies, the l_c curves for the two systems should merge. We have calculated the l_c values expected on the basis of a previous model[33,35] which assumes that

the level spacing must be less than or equal to the level width for all l values which can lead to fusion. Using the same level density (Gilbert and Cameron) and moment of inertia parameters employed previously,[35] one obtains the dashed curve in Fig. 8. It should be noted that conventional level density expressions predict that $D_J \approx \Gamma_J$ for energies not much above the yrast line when the mass number is as large as 40. To test the sensitivity of the calculated $\Gamma/D=1$ line to the level density prescription used, we have also calculated this quantity using level densities calculated[38] by the Hillman-Grover combinatorial method[38] with single-particle levels chosen by Beckerman.[39] This curve is in better agreement with the experimental data. We have also calculated l_c values using the "statistical yrast line" model of Lee *et al.*[34] This model underestimates the l_c values by about 2 units when the empirical parameters $r_0=1.2$ fm and $\Delta Q=10$ MeV are used. From these comparisons we conclude that compound nuclear level density limitations are qualitatively but not quantitatively consistent with the observations. Accurate data for the two systems at high excitation energy are required to definitively distinguish between entrance channel and compound nuclear limitation models.

V. SUMMARY

The fusion cross section excitation function has been remeasured for the $^{28}C + ^{28}Si$ system. The absolute cross sections are larger than an earlier measurement and are in qualitative agreement with entrance channel models. It is not clear whether compound nuclear limitations have come into play at the highest bombarding energies. The excitation function does not exhibit any significant structure correlated with structures observed in back-angle elastic and inelastic scattering.

ACKNOWLEDGMENTS

This work was supported in part by the U. S. Department of Energy. We thank M. Beckerman for providing us with a copy of the Hillman-Grover combinatorial code, and Harvey Wegner for performing the evaporation calculations with the CASCADE code.

---

*Present address: Max-Planck-Institut für Kernphysik, Heidelberg, West Germany.

†Present address: Institut de Physique Nucleaire, B.P. No. 1, Orsay, France.

[1]J. Barrette, M. J. LeVine, P. Braun-Munzinger, G. M. Berkowitz, M. Gai, J. W. Harris, and C. M. Jachcinski, Phys. Rev. Lett. 40, 445 (1978); J. Barrette, M. J. LeVine, P. Braun-Munzinger, G. M. Berkowitz, M. Gai, J. W. Harris, C. M. Jachcinski, and C. D. Uhlhorn, Phys. Rev. C 20, 1758 (1979).

[2]M. R. Clover, R. M. DeVries, R. Ost, N. J. A. Rust, R. N. Cherry, Jr., and H. E. Gove, Phys. Rev. Lett. 40, 1008 (1978); R. Ost, M. R. Clover, R. M. DeVries, B. R. Fulton, H. E. Gove, and N. J. Rust, Phys. Rev. C 19, 740 (1979).

[3]S. Kubono, P. D. Bond, D. Horn, and C. E. Thorn, Phys. Lett. 84, 408 (1979).

[4]R. Vandenbosch, D.-K. Lock, A. J. Lazzarini, K. Lesko, and V. Metag, Phys. Rev. Lett. 46, 5 (1981).

[5]D. Shapira, Y.-D. Chan, K. A. Erb, J. L. C. Ford, Jr., R. Novotny, J. D. Moses, and J. C. Peng, Bull. Am. Phys. Soc. 26, 611 (1981).

[6]M. Paul, S. J. Sanders, D. F. Geesaman, W. Henning, D. G. Kovar, C. Oliver, and J. P. Schiffer, Phys. Rev. C 21, 1802 (1980); S. J. Sanders, M. Paul, J. Cseh, D. F. Geesaman, W. Henning, D. G. Kover, R. Kozub, C. Olmer, and J. P. Schiffer, *ibid.* 21, 1810 (1980).

[7]T. M. Cormier, J. Applegate, G. M. Berkowitz, P. Braun-Munzinger, P. M. Cormier, J. W. Harris, C. M. Jachcinski, L. L. Lee, Jr., J. Barrette, and H. E. Wegner, Phys. Rev. Lett. 38, 940 (1977).

[8]C. M. Jachcinski, T. M. Cormier, P. Braun-Munzinger, G. M. Berkowitz, P. M. Cormier, M. Gai, and J. W. Harris, Phys. Rev. C 17, 1263 (1978).

[9]R. J. Markham, S. M. Austin, and H. Laumer, Nucl. Instrum. Methods 129, 141 (1979).

[10]L. C. Northcliffe and R. F. Schilling, Nucl. Data Tables A7, 233 (1970).

[11]A. Gavron, Phys. Rev. C 21, 230 (1980).

[12]The code PACE is a modification by A. Gavron of the code JULIAN, written by M. Hillman and Y. Eval.

[13]J. Gomez del Campo and R. Stokstad, Oak Ridge National Laboratory, report, 1981 (unpublished).

[14]F. Puhlhofer, Nucl. Phys. A280, 267 (1977).

[15]A. Gilbert and A. G. W. Cameron, Can. J. Phys. 43, 1446 (1965).

[16]W. Dilg, W. Schantl, and H. Vonach, Nucl. Phys. A217, 269 (1973).

[17]W. J. Jordan, J. V. Maher, and J. C. Peng, Phys. Rev. Lett. 87B, 38 (1979).

[18]M. Hugi, J. Lang, R. Müller, E. Ungericht, K. Bodek, L. Jarcyzk, B. Kamys, A. Magiera, A. Strakkowski, and G. Willim, Nucl. Phys. A368, 173 (1981).

[19]S. J. Sanders, M. Paul, J. Cseh, D. F. Geesaman, W.

Henning, D. G. Kovar, R. Kozub, C. Olmer, and J. P. Schiffer, Phys. Rev. C 21, 1810 (1980).
[20]S. J. Sanders, C. Olmer, D. F. Geesaman, W. Henning, D. G. Kovar, M. Paul, and J. P. Schiffer, Phys. Rev. C 22, 2914 (1980).
[21]R. Bass, Phys. Lett. 47B, 139 (1973).
[22]R. Bass, Nucl. Phys. A231, 45 (1971).
[23]J. R. Birkelund, L. E. Tubbs, J. R. Huizenga, J. N. De, and D. Sperber, Phys. Rep. 56, 107 (1979).
[24]R. Vandenbosch, Nucl. Phys. A339, 167 (1980).
[25]J. Blocki, J. Randrup, W. J. Swiatecki, and C. F. Tsang, Ann. Phys. (N.Y.) 105, 427 (1977).
[26]J. Randrup, Ann. Phys. (N.Y.) 112, 356 (1978).
[27]C. W. deJager, At. Data Nucl. Data Tables 14, 485 (1974).
[28]J. Randrup (unpublished).
[29]W. J. Swiatecki, Lawrence Berkeley Laboratory Report No. LBL-8950, 1979 (unpublished).
[30]D. G. Kovar, D. F. Geesaman, T. H. Braid, Y. Eisen, W. Henning, T. R. Ophel, M. Paul, K. E. Rehm, S. J. Sanders, P. Sperr, J. P. Schiffer, S. L. Tabor, S. Vigdor, B. Zeidman, and F. W. Prosser, Jr., Phys. Rev. C 20, 1305 (1979).
[31]M. Conjeaud, S. Gary, S. Harar, and J. P. Wieleczko, Nucl. Phys. A309, 515 (1978).
[32]F. Saint-Laurent, M. Conjeaud, S. Harar, J. M. Loiseaux, J. Menet, and J. B. Viano, Nucl. Phys. A327, 517 (1979).
[33]R. Vandenbosch, Phys. Lett. 87B, 183 (1979).
[34]S. M. Lee, T. Matsuse, and A. Arima, Phys. Rev. Lett. 45, 165 (1980).
[35]R. Vandenbosch and A. J. Lazzarini, Phys. Rev. C 23, 1074 (1981).
[36]S. M. Lee, Y. Higashi, Y. Nagashima, S. Hanashima, M. Sato, H. Yamaguchu, M. Yamanouchi, and T. Matsuse, Phys. Lett. 98B, 418 (1981).
[37]S. L. Tabor, D. F. Geesaman, W. Henning, D. G. Kovar, K. E. Rehm, and F. W. Prosser, Jr., Phys. Rev. C 17, 2136 (1978).
[38]M. Hillman and J. R. Grover, Phys. Rev. 185, 1303 (1969).
[39]M. Beckerman, Nucl. Phys. A278, 333 (1977).